

**Fast Access to Neutral Injection
Heating Profiles in W7AS**

Franz-Peter Penningsfeld

IPP 4/265

November 1993



MAX-PLANCK-INSTITUT FÜR PLASMAPHYSIK

85748 GARCHING BEI MÜNCHEN

**MAX-PLANCK-INSTITUT FÜR PLASMAPHYSIK
GARCHING BEI MÜNCHEN**

**Fast Access to Neutral Injection
Heating Profiles in W7AS**

Franz-Peter Penningsfeld

IPP 4/265

November 1993

*Die nachstehende Arbeit wurde im Rahmen des Vertrages zwischen dem
Max-Planck-Institut für Plasmaphysik und der Europäischen Atomgemeinschaft über
die Zusammenarbeit auf dem Gebiete der Plasmaphysik durchgeführt.*

Fast Access to Neutral Injection Heating Profiles in W7AS

F.-P. Penningsfeld

Abstract

A fast code was developed to estimate the heating power profiles of the neutral injection system for diagnosed shots of W7AS. This code, named NIPOR, uses a number of data sets of the local power deposition of neutral beams and analytical fits of the total heating efficiency for each source. These data were obtained by previous runs of FAFNER1, a Monte Carlo code for simulating the NI heating on W7AS.

The main input parameters needed for this estimation are the electron density $n_e(r)$, electron temperature $T_e(r)$, toroidal magnetic field B_0 and the identifiers of the active NI-sources at the corresponding time t_c . These data are routinely read from the ORACLE data set.

To achieve high flexibility of the available FAFNER1 data, the heating profiles were not stored direct, but in the form of radially deposited heating power per source as a function of the normalized variable $\xi(r)$, defined as the line-integrated density from the plasma edge to the centre divided by the the volume of the corresponding shell. The variable $\xi(r)$ is normalized to $0 < \xi(r) < 1$. The partition of the reconstructed heating profile $p_{\text{heat}}(r)$ to heating of the ions $p_i(r)$ and electrons $p_e(r)$ is then estimated by using the critical energy $E_{\text{crit}}(r)$ as a function of $T_e(r)$. The influence of neutral gas on the global heating efficiency at low density target plasmas via charge exchange losses is also included.

Table of contents

1) Introduction	...2
2) Reconstruction of the heating profile	...5
3) Estimation of the ion/electron heating	...9
4) Global heating efficiencies	..10
5) Additional parameters	
a) Combined heating with ECRH	..13
b) Influence of the neutral gas	..14
6) Comparison with FAFNER1 results	..16
References	..20
Appendix : data sets used	..21

1) Introduction

The **NIPOR** (Neutral Injection Power using **ORACLE** data base) program is a fast method of estimating the NI heating profiles $p_{i,e,total}(r_{eff})$ for shots listed in **ORACLE**, at times when electron density and temperature profiles were measured and stored. The results are given in the form of a plot with listing and an output file for further use.

NIPOR is based on a large number of results of the MONTE CARLO code, FAFNER1, for the NI heating system on W7AS with two sources firing in the CO and two sources firing in the COUNTER direction (see Table 1 and Fig.1). The data of the heating sources are read from **ORACLE** and, if $n_e(r)$, $T_e(r)$ data at time t_c are available, the actual source combination at t_c is identified.

The basic idea for achieving high flexibility in the application of the available FAFNER1 data is to transform the calculated power density profiles for some typical target plasmas into normalized heating power profiles $P_j(\xi)$ for each source j , where ξ is defined by the line density from the edge a to the effective radius r , divided by the corresponding volume of the plasma cross-section. In this way, the NI heating profiles for a wide range of plasma profiles can be computed rather quickly with an acceptable degree of accuracy within less than 5 sec CPU time on the IBM compared with about 2 hours for FAFNER1 runs on the CRAY.

Table 1: List of NI sources available on W7AS in phase 1

name	short name	ID
outer west	WBL1	1
inner west	WBL3	3
inner east	OBL1	5
outer east	OBL3	7

The application of NIPOR in a wide field of plasma parameters and comparison with additional FAFNER1 runs resulted in the inclusion of some additional parameters to get satisfactory agreement. The list of parameters actually implemented is given in Table 2.

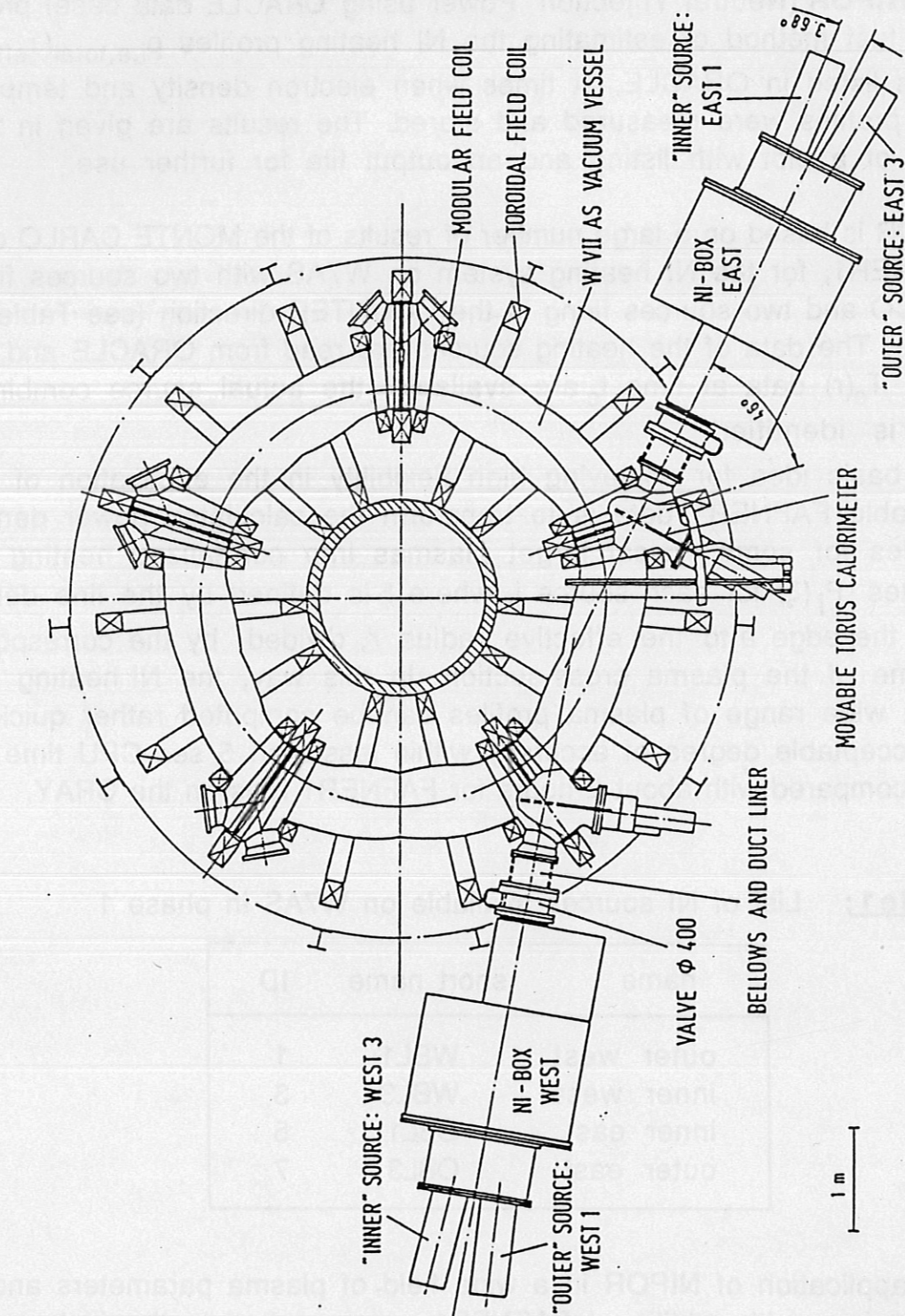


Fig.1: Top view of the NBI system for W7AS. In phase 1 two NI sources are mounted on each box at the positions indicated.

Table2: List of parameters used in NIPOR

parameter	meaning	range	comment
$n_e(r)$	electron density [$10^{20}m^{-3}$]	0.2 --> 3.0	read from ORACLE
$T_e(r)$	electron temperature [keV]	0.150 --> 2.500	read from ORACLE
t_c	profile recording time [sec]		read from ORACLE
B_0	toroidal field [tesla]	1.25 , 2.50	read from ORACLE
j	active source identifier		read from ORACLE
$P_{day,j}$	day factor per source j	0.90 --> 1.20	input (default: 1.0)
$n_0(a)$	neutral density on edge [$10^{10}cm^{-3}$]	0.5 --> 2.5	input (default: 2.0)

In standard application all these parameters are obtained from the ORACLE data base with the exception of the day-factor of the sources and the density $n_0(a)$ of the neutral gas on the plasma edge, depending on the vessel condition. Results of the DEGAS code show typically $1.0 < n_0(a) < 2.0 \times 10^{10} cm^{-3}$, hence the default value in NIPOR is 2.0.

The influence of a radial electric field E_{rad} on the fast ion orbits, which in turn can modify the local and global NI heating, was studied earlier /2,3/. It was found that for W7AS the NI heating is nearly independent of E_{rad} because the tangential injection generates the fast ions far away from the loss cone /4/. The radial electric field is therefore not included in the actual parameter list of NIPOR.

The topology of the magnetic field is given in a 3D grid for standard rotational transform $\chi = 0.38$, scaled by B_0 . The influence of χ on the NI heating profiles has not been included up to now.

In section 2, the evaluated method of reconstructing the heating profiles for actual shots from the FAFNER1 data sets is described in more detail. Section 3 contains the estimation of the ion/electron heating from the total heating density profile, and section 4 the analytical representation of the global heating efficiencies.

In section 5 two additional parameters for expanding the code to a

larger range of plasma parameters are described: the influence of the neutral gas $n_0(a)$ on charge exchange losses at low densities and the variation of the heating efficiency by the high electron temperatures T_e obtained in NI+ECRH heated discharges.

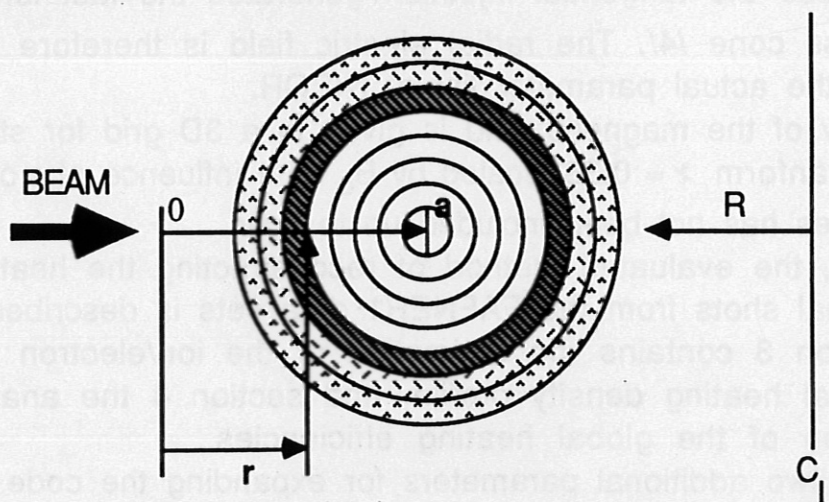
Some examples of the application of NIPOR are given in section 6 and the results of this fast estimation are compared with explicit FAFNER1 runs, which are not included in the data set.

2) Reconstruction of the heating profile

For a fast estimation of the global and local plasma heating by the neutral beams in a wide range of plasma density profiles $n_e(r)$, results of the FAFNER1 Monte Carlo program are used to create a data set as a function of the normalized variable $0 < \xi(r) < 1$, defined by the line density from the edge $r=0$ to the effective radius r , divided by the corresponding volume of the plasma cross-section:

$$(1) \quad \xi(r) \equiv \frac{\int_0^r n \, dl : \int_0^r dV}{\int_0^a n \, dl : \int_0^a dV}$$

In this way the variable $\xi(r)$ combines both the line-integrated density from edge to centre, which is responsible for the beam absorption, and the different volume of the toroidal shells, which is needed to calculate the local heating power density.



Heating power profiles given as a function of this variable ξ are more flexible for application to plasma targets with different density profiles $n_e(r)$. These profiles $P_j(\xi)$ were therefore calculated from a lot of FAFNER1 results for each source j , normalized to $\int P_j(\xi) d\xi = 1$ and stored as input data set for NIPOR (see Appendix).

To reconstruct the actual heating profile for a given density profile $n_e(r)$ of the target plasma, read in from ORACLE with a radial resolution of $\Delta = 1$ cm, the normalized variable $\xi(r)$ (eq. 1) for this profile is calculated.

The normalized heating power $P_j(\xi)$, given for five sets of central densities $n_e(0)$, is then interpolated to $\langle P_j(\xi) \rangle$, in accordance with the actual central density of the plasma target. The power deposition per source is then

$$(2) \quad P_{\text{norm},j}(r_{\text{eff}}) = \langle P_j(\xi) \rangle \quad \text{renormalized to} \quad \int P_{\text{norm},j}(r_{\text{eff}}) dr_{\text{eff}} = 1.$$

and describes the radial heating profile in relative units. The heating in absolute units is obtained by multiplying this profile by the heating efficiency η_j (see section 4) and the standard neutral power per source $P_0 = 375$ kW:

$$(3) \quad P_{\text{heat},j}(r_{\text{eff}}) = P_0 \eta_j(\int n dl, n_0(a)) P_{\text{norm},j}(r_{\text{eff}}) \quad [\text{W}].$$

The estimated heating power density $p_{\text{heat}}(r_{\text{eff}})$ is the sum over all sources j active at this moment, divided by the local volumes of the corresponding plasma shell:

$$(4) \quad p_{\text{heat}}(r_{\text{eff}}) = \sum_j P_{\text{heat},j}(r_{\text{eff}}) / V(r_{\text{eff}}) \quad [\text{W}/\text{cm}^3],$$

$$(5) \quad V(r_{\text{eff}}) = 2 R_0 \pi^2 (r_a^2 - r_b^2) \quad \text{with} \quad r_{a,b} = r_{\text{eff}} \pm 1 \quad [\text{cm}].$$

An example of this method is shown in Fig. 2a-d for two different target plasmas heated by one source (OBL1). In order to obtain sufficient accuracy, the radial resolution in the dimension of ξ is a factor of two higher than the effective radius r_{eff} .

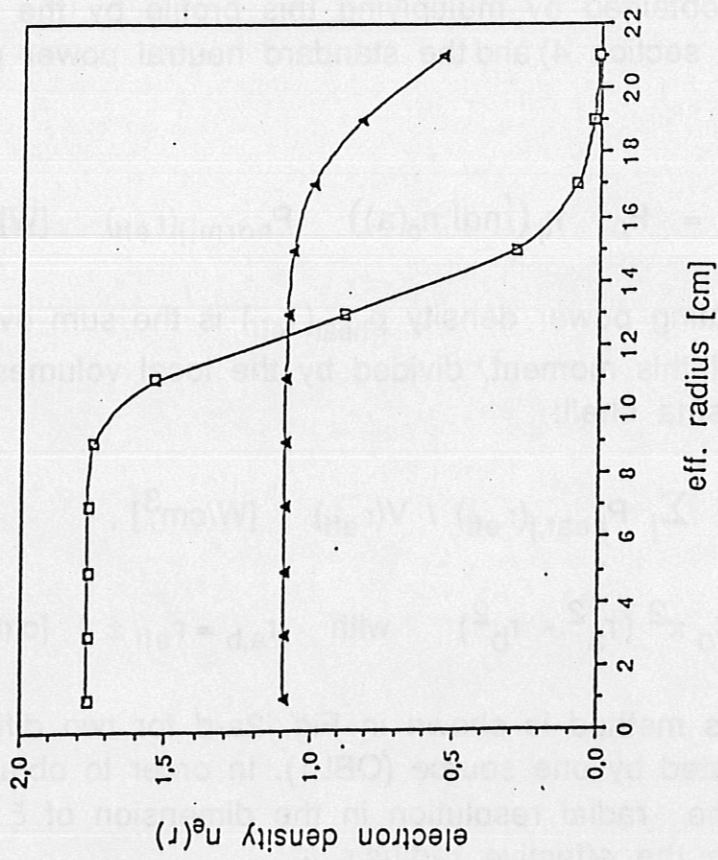


Fig.2a: Two examples of density profiles with $\int n_{\text{eff}} \approx \text{const.}$

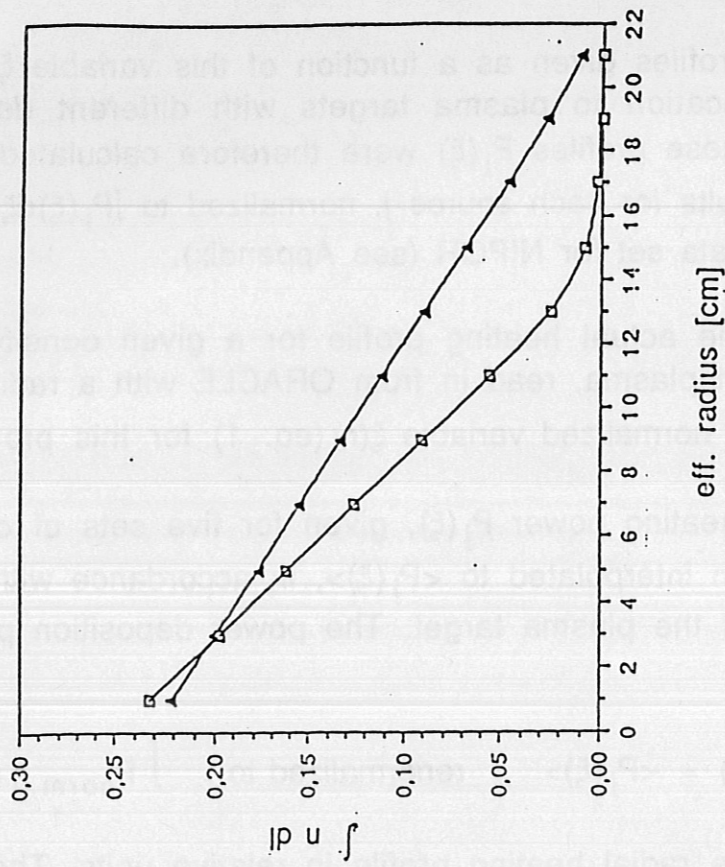


Fig.2b: $\int n_{\text{eff}}$ from edge to centre as used to calculate $\xi(r_{\text{eff}})$ shown in Fig.2d.

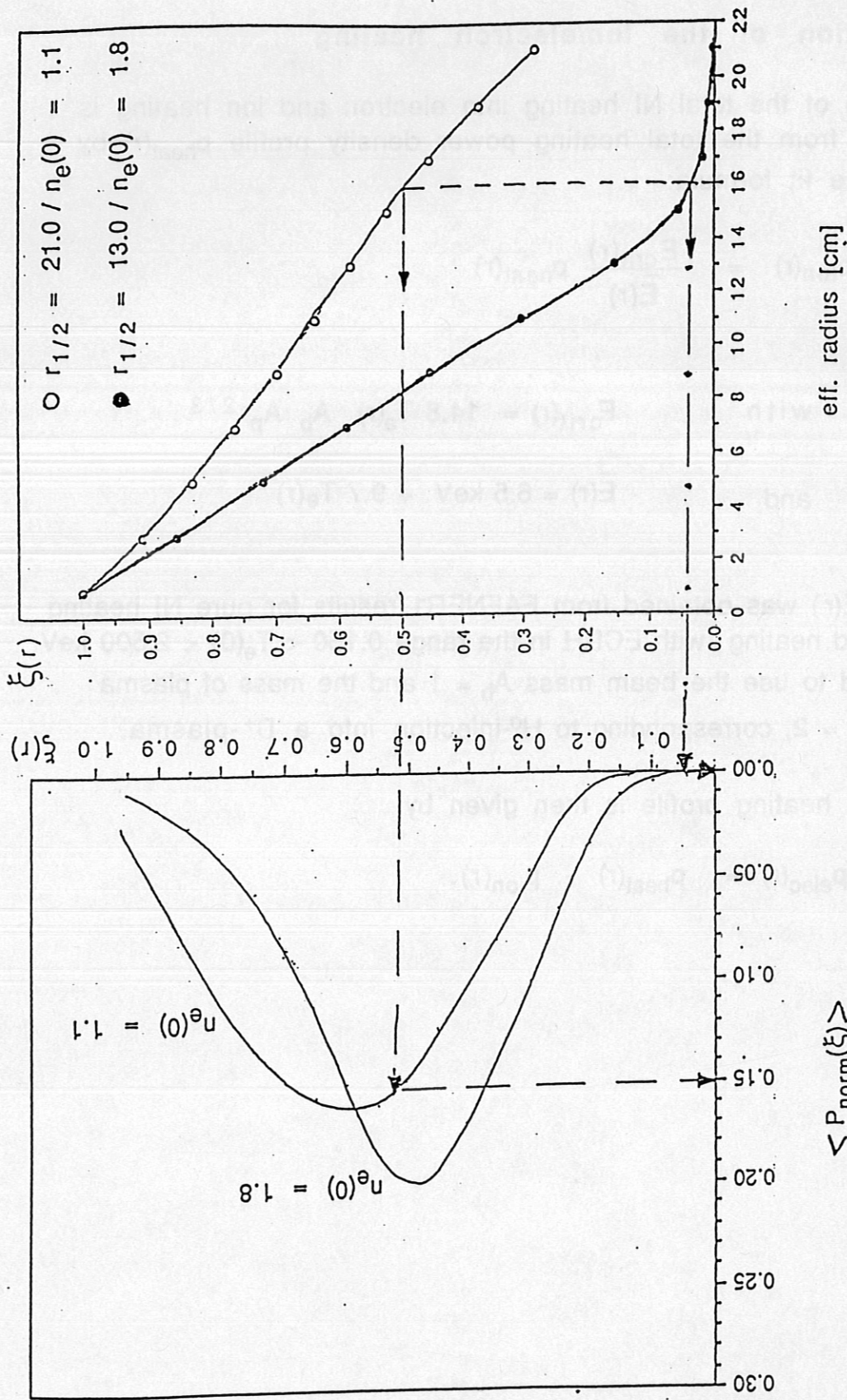


Fig. 2c: Normalized heating power of source OBL1 obtained from the data sets for the two target densities $n_{\theta}(0)$. The arrows indicate the heating power $\langle P_j(\xi) \rangle$ used locally to reconstruct $P_{\text{norm},j}(r_{\text{eff}})$.

Fig. 2d: Normalized variable $\xi(r_{\text{eff}})$ for the two profiles of Fig. 2a.

3) Estimation of the ion/electron heating

The partition of the total NI heating into electron and ion heating is recalculated from the total heating power density profile $p_{\text{heat}}(r)$ by means of the fit formula:

$$(6) \quad p_{\text{ion}}(r) = \frac{E_{\text{crit}}(r)}{\bar{E}(r)} p_{\text{heat}}(r)$$

$$\text{with} \quad E_{\text{crit}}(r) = 14.8 T_e(r) A_b A_p^{-2/3}$$

$$\text{and} \quad \bar{E}(r) = 6.5 \text{ keV} + 9.7 T_e(r)$$

The fit for $E(r)$ was obtained from FAFNER1 results for pure NI heating and combined heating with ECRH in the range $0.150 < T_e(0) < 2.500$ keV. It is standard to use the beam mass $A_b = 1$ and the mass of plasma particles $A_p = 2$, corresponding to H^0 -injection into a D^+ -plasma.

The electron heating profile is then given by

$$(7) \quad p_{\text{elec}}(r) = p_{\text{heat}}(r) - p_{\text{ion}}(r).$$

4) Global heating efficiencies

The global heating efficiency of each source on W7AS was calculated over a wide range of line density of the target plasma by means of the NI simulation code FAFNER1. For the scan in line density, a typical measured density profile was used and varied in line density by varying the central density $n_e(0)$ only. These scans were done for full magnetic field (2.5 T; example: #15021) and for half field (1.25 T; example: #17916).

The FAFNER1 results for the heating efficiencies were then fitted for each source j by /5/

$$(8) \quad \eta_j^0 = A_{3,j} \sum_{k=1}^3 s_k \left(1 - e^{-\sigma_k A_{1,j} (n_e - A_{4,j})} \right) e^{-\sigma_k n_e A_{2,j}}$$

with mean density

$$n_e \equiv \frac{\int n dl_{\text{eff}}}{2 \bar{a}}$$

The sum \sum_k adds the three species k of each beam with different cross-sections σ_k of the neutral beam species mix given by s_k . The beam parameters s_k and σ_k are set in the EFFHEAT subroutine as well as the parameter sets $A_{m,j}$ ($m=1,4$) of these fits, given for both values of the magnetic field.

The FAFNER1 results are shown in Fig. 3a-d for each source together with the corresponding analytic fits for η_j^0 . The difference is mainly caused by the different positions of these CO, COUNTER, INNER and OUTER sources and their influence on the orbits of the injected particles. The difference of η_j^0 between full and half field target is only significant for counter beams (WBL1,WBL3).

For low-density targets charge exchange losses strongly increase and are described by the parameter $n_0(a)$ (see section 5b), which had the standard value $2.0 \times 10^{10} \text{ cm}^{-3}$ in this data set. In view of such CX losses and shinethrough losses the lowest accepted heating efficiency was set at $\eta_{j,\text{min}}^0 = 0.30$. At lower values the program stops to avoid excessive errors.

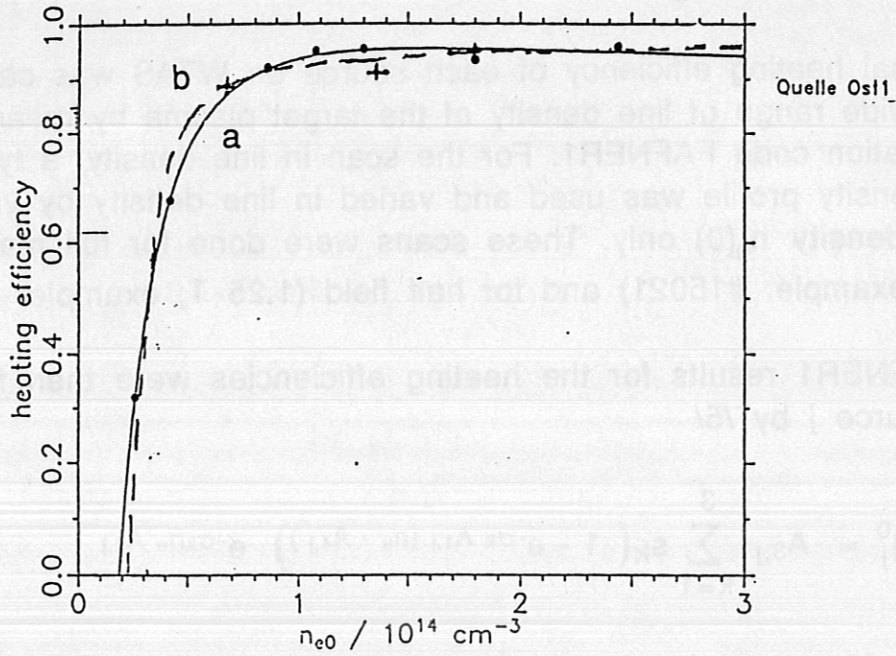


Fig.3a: Fits of the calculated heating efficiencies for source OBL1 (co, inner) for magnetic field $B_0=2.5$ T (a) and $B_0=1.25$ T (b).

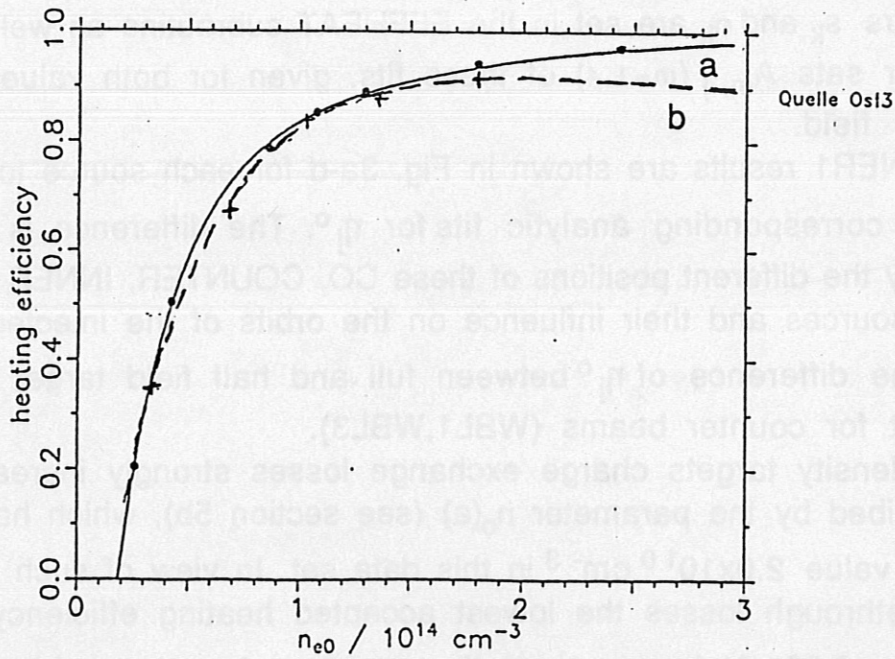


Fig. 3b: Calculated heating efficiencies for source OBL3 (co, outer)

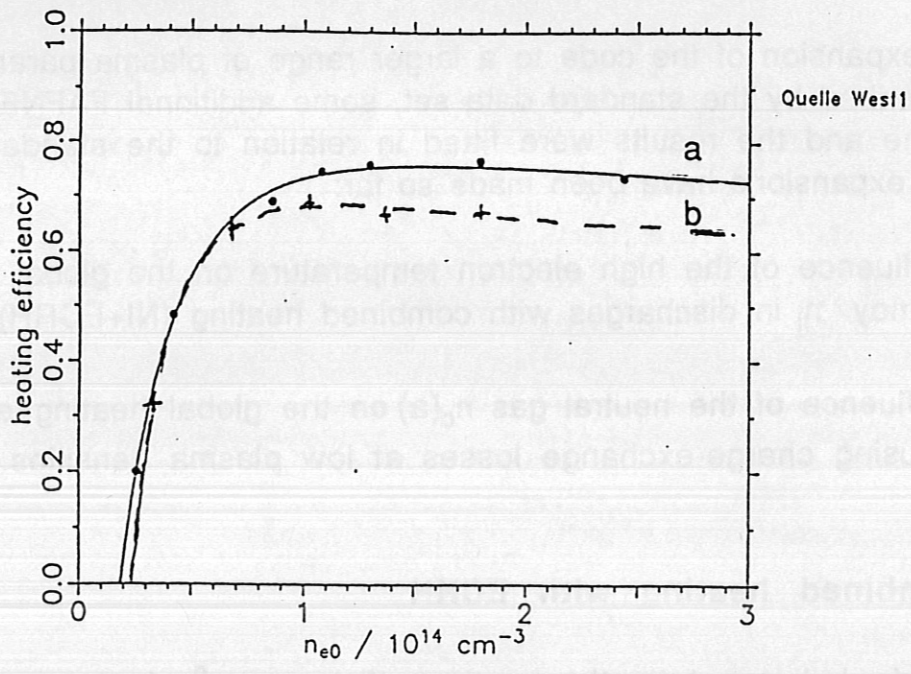


Fig. 3c: Fit of the calculated heating efficiency for source WBL1 (counter, outer) for magnetic field $B_0=2.5$ T (a) and $B_0=1.25$ T (b).

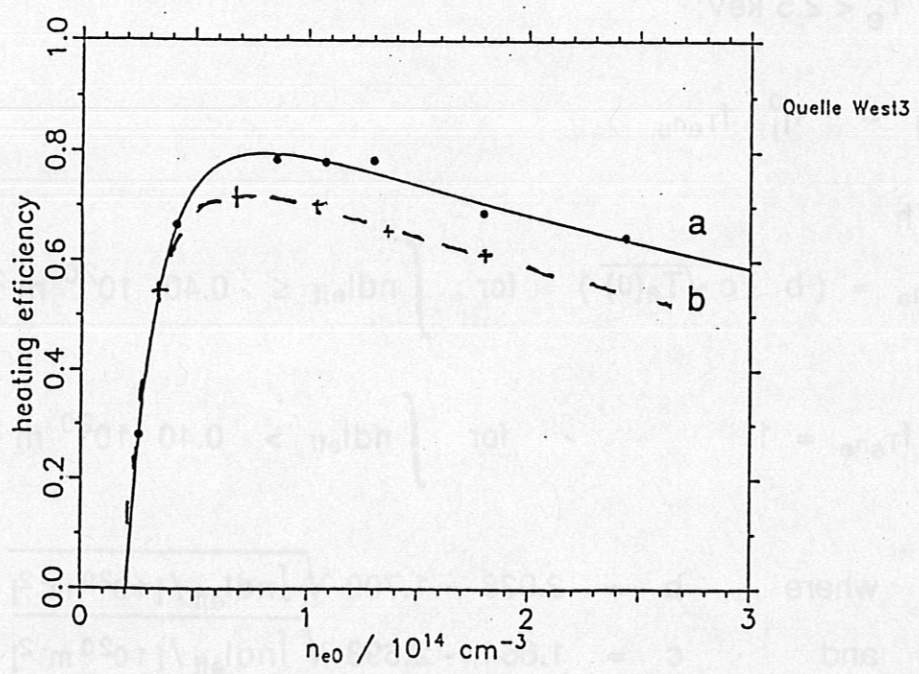


Fig 3d: Calculated heating efficiencies for source WBL3 (counter, inner)

5) Additional parameters

For the expansion of the code to a larger range of plasma parameters than described by the standard data set, some additional FAFNER1 runs were done and the results were fitted in relation to the standard data set. Two expansions have been made so far:

- a) the influence of the high electron temperature on the global heating efficiency η_j in discharges with combined heating (NI+ECRH) and
- b) the influence of the neutral gas $n_0(a)$ on the global heating efficiency η_j , causing charge-exchange losses at low plasma densities.

5a) Combined heating with ECRH

The standard data set for the heating efficiency η_j^0 of source j was calculated for $0.35 < T_e(0) < 0.55$ keV. For an application of NIPOR to higher electron temperatures, in NI+ECRH-heated discharges, for example, a fit formula was derived from the results of some special FAFNER1 runs to describe the temperature dependence of η_j in the range $0.2 \text{ keV} < T_e < 2.5 \text{ keV}$:

$$(9) \quad \eta_j = \eta_j^0 f_{T_e n_e}$$

with

$$(10) \quad f_{T_e n_e} = (b - c \sqrt{T_e(0)}) \quad \text{for} \quad \int n d l_{\text{eff}} \leq 0.40 \cdot 10^{20} \text{ m}^{-2},$$

$$f_{T_e n_e} = 1 \quad \text{for} \quad \int n d l_{\text{eff}} > 0.40 \cdot 10^{20} \text{ m}^{-2},$$

$$\text{where} \quad b = 2.038 - 1.700 \sqrt{\int n d l_{\text{eff}} / [10^{20} \text{ m}^{-2}]},$$

$$\text{and} \quad c = 1.664 - 2.693 \sqrt{\int n d l_{\text{eff}} / [10^{20} \text{ m}^{-2}]}.$$

η_j^0 describes the efficiency calculated for the standard target

discharge as stored in the data set. The factors b and c depend again on the line density because the slowing-down times of fast ions are strongly increased for low-density targets and this fact in turn increases charge-exchange losses, which means it decreases the global heating efficiency.

5b) Influence of the neutral gas

The influence of the neutral gas density $n_0(a)$ at the plasma edge on the heating efficiency of the beams is included in FAFNER1 by a three-dimensional estimation of the neutral gas $n_0(R,\varphi,z)$ penetrating into the actual plasma described by the 3D n_e -profile.

Figure 4 shows the reduction of η_j with increasing $n_0(a)$ for various central electron densities $n_e(0)$. Especially at lower densities, this means $n_e(0) < 1 \times 10^{20} \text{ m}^{-3}$, $n_0(a)$ shows an increasing influence on η_j . The results for calculated CX losses could be coarsely fitted in the two dimensional range $\{n_e(0), n_0(a)\}$ for $0.7 < n_0(a) < 2.5$ and $0.2 < n_e(0) < 2.0$ ($n_0(a)$ in 10^{10} cm^{-3} and $n_e(0)$ in 10^{14} cm^{-3}) by

$$(11) \quad \eta_j = \eta_j^0 f_{CX} \quad \text{with}$$

$$(12) \quad f_{CX} = (c_1 + c_2 n_0(a)) (c_3 + c_4 \exp(-c_5 n_e(0)))$$

with the parameters

(13)	$c_1 = -0.052$	$c_2 = 0.526$	for $B = 1.25 \text{ T}$
	$c_1 = 0.323$	$c_2 = 0.338$	for $B = 2.50 \text{ T}$

and

	c_3	c_4	c_5
(14) B (tesla):	1.25 2.50	1.25 2.50	1.25 2.50
inner sources:	0.03 0.06	2.7 15.8	7.54 10.00
outer sources:	0.02 0.04	0.8 10.8	4.70 9.60

f_{cx} describes a linear variation of the CX losses with $n_0(a)$, and projects the exponential variation of CX losses with $n_e(0)$, calculated by FAFNER1, in the range of the actually assumed neutral gas parameter $n_0(a)$. This fit is used in NIPOR if $n_0(a)$ is given explicitly ($n_0(a) = 2.0 \times 10^{10} \text{ cm}^{-3}$ is standard).

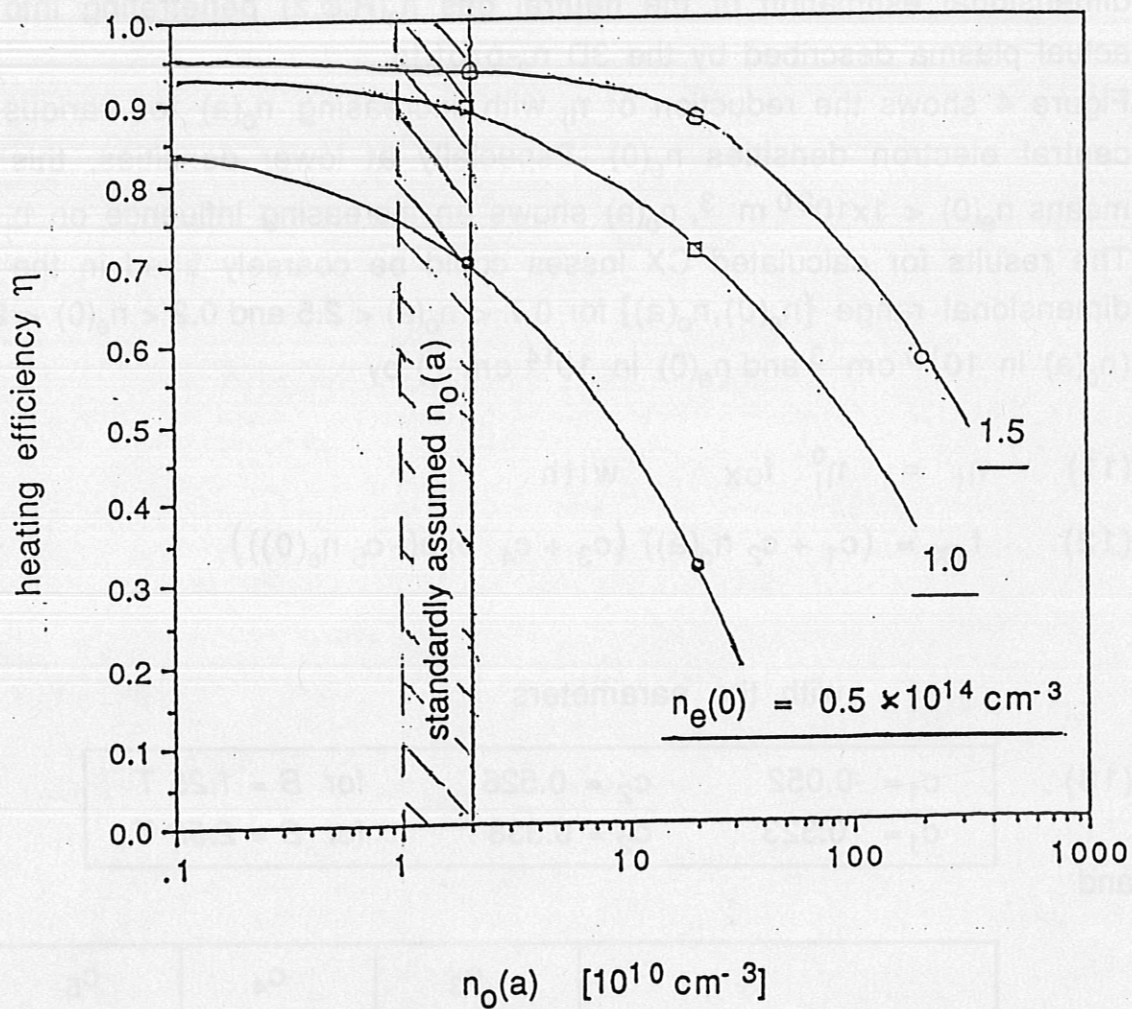


Fig. 4: Influence of the CX losses on the heating efficiency η of source OBL1 by the neutral gas density at the edge $n_0(a)$. η is strongly reduced for targets with $n_e(0) < 10^{14} \text{ cm}^{-3}$ and $n_0(a) > 2 \times 10^{10} \text{ cm}^{-3}$

6) Comparisons with FAFNER1 results

The application of NIPOR (or NIPOW, a version of NIPOR using Gauss- or Lorentz-type fits for T_e and n_e instead of the data sets read from ORACLE) was tested for a lot of NI heated W7AS discharges by additional FAFNER1 runs for these shots. This means that the FAFNER1 results of these runs were not included in the data set used in NIPOR.

Three examples are shown in Fig. 5,a,b,c, where the estimated heating profiles are compared with the elaborate calculations of FAFNER1 (indicated by crosses for p_{heat} and triangles for p_{ion}).

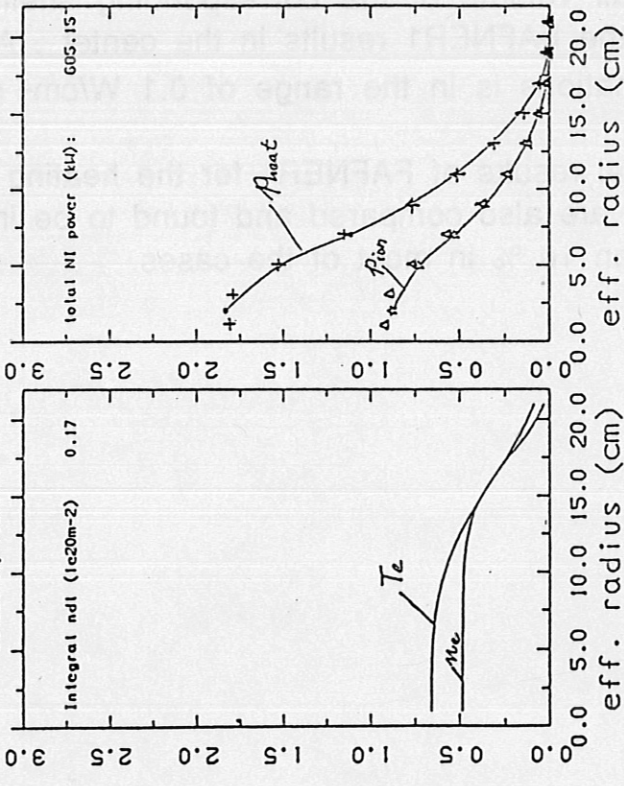
Very good consistency is obtained. Nevertheless, a difference of up to 25% in the inner part ($r_{\text{eff}} < 0.05$ m) may occur, this being caused by the very small volume of the corresponding shell and the larger statistical error of the FAFNER1 results in the center. An absolute error bar for the estimations is in the range of 0.1 W/cm^3 over the whole radius.

The global results of FAFNER1 for the heating power to ions and electrons are also compared and found to be in very good agreement, better than 10 % in most of the cases.

IPP--LMS FPP /0001 62-08 15.07.93 15.13:18
 15.07.93 15.12:45

ESTIMATED NI POWER PROFILE / FPP VERSION 9

ne(r): GAUSS-profile with parms 1-6 : 0.000 0.404 17.330 7.154 0.000 0.000
 Te(r): GAUSS-profile with parms 1-6 : 0.000 0.659 15.050 3.705 0.000 0.000
 List of assumed active sources : WBL3 OBL1 OBL3
 actual day factor : 1.00 1.00 1.00



SHOT : 14993.
 t(s) : 0.200

r	ne	Te	pheat	pion
1.0	0.404	0.659	1.070	0.099
3.0	0.404	0.659	1.706	0.054
5.0	0.404	0.653	1.519	0.724
7.0	0.403	0.639	1.110	0.523
9.0	0.401	0.607	0.779	0.350
11.0	0.471	0.554	0.523	0.228
13.0	0.443	0.475	0.320	0.132
15.0	0.378	0.375	0.174	0.060
17.0	0.265	0.267	0.050	0.016
19.0	0.127	0.166	0.000	0.002
21.0	0.031	0.000	0.000	0.000

B (Testa) : 2.56
 no(a) (10**10 cm-3) : 2.00
 nd1 (10**16 cm-2) : 0.17

FAF1	
305	+0.3%
376	-0.4%
681	+0.6%

power to ions (kw) : 306.
 to electrons : 379.
 total heating power : 605.

Fig. 5a: Comparison of FAFNER1 results with the NIPOW estimation for shot 14993, heated by sources WBL3,OBL1 and OBL3 at the time $t_c = 0.200$ s. T_e - and n_e -profile were fitted by GAUSS profiles, with the parameters 1-6 listed on the plot.

IPP--CMS FPP

/0001

B2-08

15.07.93

15.01:25

15.07.93 15.00:30

ESTIMATED NI POWER PROFILE / FPP VERSION 9

ne(r): LORENTZ-profile with parms 1-6:

Te(r): LORENTZ-profile with parms 1-6:

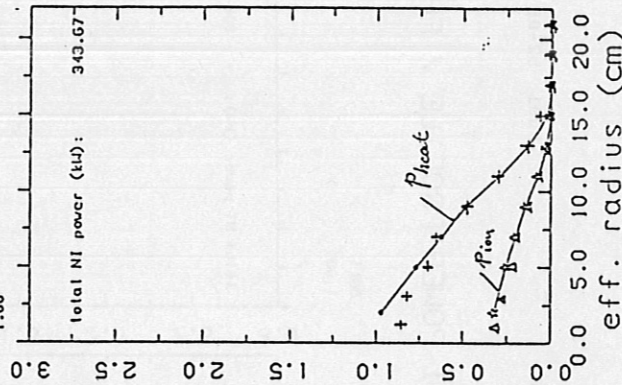
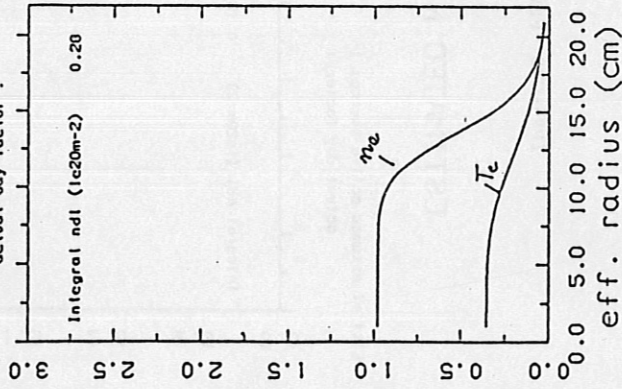
List of assumed active sources :

actual day factor :

0.000 0.900 13.000 4.110 0.000 0.000
 0.000 0.352 12.940 2.313 0.000 0.000

OBL1

1.00



SHOT : 11387.
 t(s) : 0.250

reff	ne	Te	pheat	pion
1.0	0.900	0.352	1.024	0.341
3.0	0.900	0.352	0.915	0.304
5.0	0.900	0.340	0.760	0.254
7.0	0.970	0.333	0.622	0.199
9.0	0.950	0.297	0.402	0.143
11.0	0.063	0.239	0.297	0.075
13.0	0.616	0.174	0.136	0.027
15.0	0.310	0.110	0.026	0.004
17.0	0.134	0.070	0.002	0.000
19.0	0.055	0.051	0.000	0.000
21.0	0.024	0.034	0.000	0.000

B (Testo) : 2.50
 no(a) (10**10 cm-3) : 2.00
 nd1 (10**16 cm-2) : 0.20

power to ions (kW) : 102.
 to electrons : 242.
 total heating power: 344.

FAF1	
3I	+4.2
250	-3.22
348	-6.12

Fig.5b: Comparison of FAFNER1 results with the NIPOW estimation for shot 11387, heated only by OBL1 at the time $t_c = 0.250$ s. T_e - and n_e -profiles were fitted by LORENTZ profiles, with the parameters 1-6 listed on the plot.

04.11.93 15:51:20
04.11.93 15:10:31

/0001 B2-08

IPP--CMS FPP

ESTIMATED NI POWER PROFILE / FPP - ORAC 2

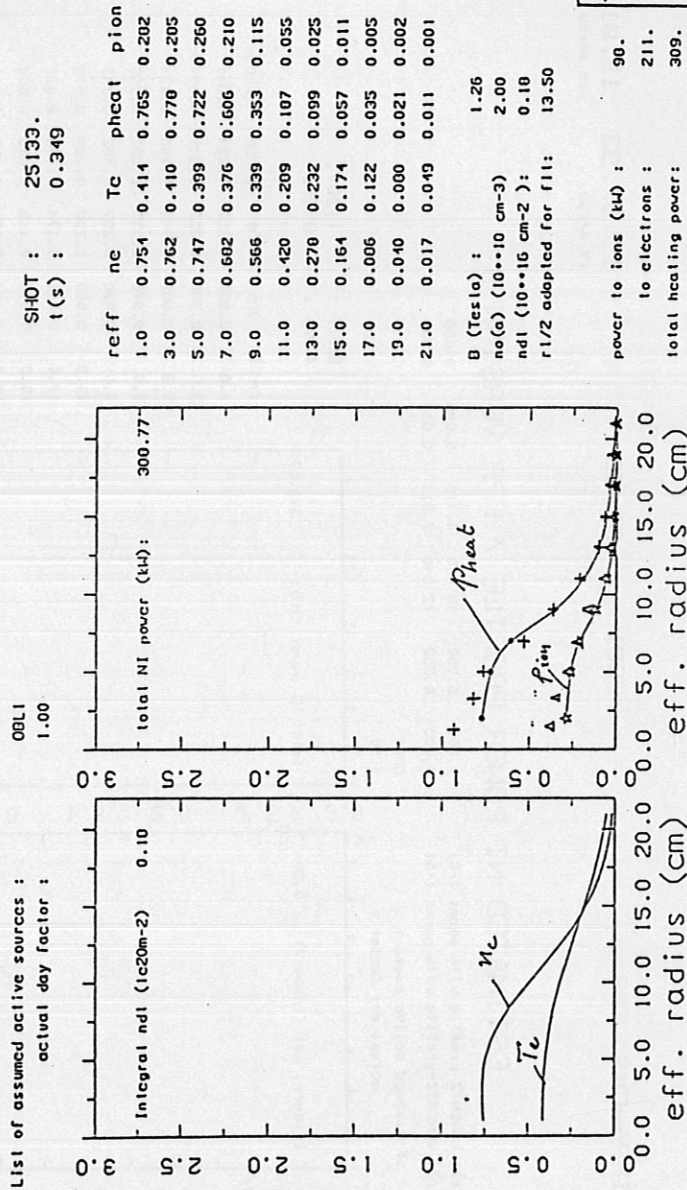


Fig. 5c: Comparison of FAFNER1 results with the NIPOW estimation for shot 25133, available in ORACLE at this time. The W7AS plasma was heated at this time $t_c = 0.349$ s by OBL1 only. The plasma parameters as well as the other data (see table 1) were obtained from ORACLE direct.

References

- [1] *Lister G.G*
FAFNER: A fully 3-D neutral beam injection code using Monte Carlo methods,
IPP/Report 4/222, Garching (1985)
- [2] *K Hanatani, F.-P. Penningfeld*
Resonant superbanana and resonant banana losses of injected fast ions in Heliotron-E and W7a: effects of the radial electric field
Nuclear Fusion, vol.32, No.10 (1992)
- [3] *A. Teubel, F.-P. Penningfeld*
Influence of the electric field on the heating efficiency in the W7AS stellarator
Proc. 19th EPS. Conf. on Plasma Phys., vol.16c, part 1, pp537, Innsbruck(1992)
- [4] *A. Teubel, F.-P. Penningfeld*
Collisionless fast ion confinement and computed heating efficiency in stellarators - a comparative study of W7a, W7AS and W7X
Proc. 20th EPS Conf. Contr. Fus & Plasma Phys., vol.17c, part 1, pp401, Lisbon(1993)
- [5] *W. Ott*
Analytic fit to the calculated heating efficiencies of the W7AS/Nl-sources (*private communication*)

Appendix

The data sets used in NIPOW/NIPOR are listed on the following pages. They contain P_{norm} for all four active sources (O1,O3,W1,W3) of the NI system on W7AS /phase1 for 20 points of the normalized variable $\xi(r)$.

Sections 1 to 5 refer to the full field results of FAFNER1 (2.5 tesla), sections 6 to 10 to the half field.

NI-W7AS / Daten zur Parametrisierung der Heizprofile

Ho -> D+ / 45 keV / 2.5 Tesla / status: 30.11.92 ---> 1. Teil

Ho -> D+ / 45 keV / 1.25 Tesla / status: 8.12.92 ---> 2. Teil

DATA : normalized Pheat versus normalized ndl/Fi for O1,O3,W1,W3

1.) $n_e(0) = 0.30 \cdot 10^{14} \text{ cm}^{-3}$ / 2.50 T

reff-Param
0.176
ne(0)-Param
0.30

norm. ndl/Fi	O1	O3	W1	W3
0.05	.0000	.0000	.0000	.0000
0.10	.0023	.0000	.0010	.0023
0.15	.0045	.0030	.0023	.0057
0.20	.0114	.0136	.0136	.0114
0.25	.0204	.0250	.0250	.0205
0.30	.0341	.0410	.0409	.0341
0.35	.0500	.0568	.0568	.0450
0.40	.0636	.0727	.0682	.0614
0.45	.0795	.0910	.0750	.0750
0.50	.0932	.1090	.0841	.0932
0.55	.1090	.1295	.1023	.1090
0.60	.1318	.1522	.1364	.1318
0.65	.1568	.1705	.1636	.1568
0.70	.1795	.1932	.1841	.1795
0.75	.1932	.1931	.1932	.1932
0.80	.1932	.1750	.1932	.1932
0.85	.1750	.1430	.1818	.1750
0.90	.1477	.1090	.1477	.1477
0.95	.1023	.0750	.0977	.1023
1.00	.0568	.0450	.0523	.0568

2.) $n_e(0) = 0.42 \cdot 10^{14} \text{ cm}^{-3}$ / 2.5 T

reff-Parameter
0.176
Param
0.42

norm. ndl/Fi	O1	O3	W1	W3
0.05	.0000	.0000	.0000	.0000
0.10	.0000	.0000	.0000	.0023
0.15	.0023	.0045	.0001	.0068
0.20	.0068	.0182	.0068	.0091
0.25	.0136	.0432	.0216	.0227
0.30	.0227	.0523	.0364	.0386
0.35	.0341	.0727	.0523	.0727
0.40	.0477	.0909	.0682	.0955
0.45	.0659	.1091	.0841	.1181
0.50	.0840	.1250	.1091	.1363
0.55	.1136	.1410	.1318	.1522
0.60	.1500	.1500	.1523	.1590
0.65	.1770	.1636	.1659	.1648
0.70	.2000	.1727	.1773	.1636
0.75	.2090	.1750	.1682	.1614
0.80	.2045	.1730	.1432	.1522
0.85	.1886	.1500	.1227	.1295
0.90	.1500	.1136	.0977	.0909
0.95	.1023	.0704	.0682	.0591
1.00	.0568	.0386	.0432	.0341

3.) $n_e(0) = 1.00 \cdot 10^{14} \text{ cm}^{-3}$ / 2.5 T

norm. n _{d1} /F _i	O1	O3	W1	W3	reff-Param 0.176 ne(0)-Param 1.00
0.05	.0000	.0000	.0000	.0000	
0.10	.0000	.0000	.0000	.0023	
0.15	.0023	.0022	.0023	.0068	
0.20	.0090	.0057	.0068	.0318	
0.25	.0255	.0159	.0205	.0659	
0.30	.0455	.0318	.0455	.1000	
0.35	.0800	.0545	.0795	.1318	
0.40	.1022	.0727	.1205	.1455	
0.45	.1272	.0955	.1455	.1545	
0.50	.1480	.1204	.1545	.1545	
0.55	.1680	.1455	.1591	.1523	
0.60	.1680	.1660	.1568	.1477	
0.65	.1680	.1727	.1523	.1432	
0.70	.1610	.1727	.1466	.1364	
0.75	.1500	.1660	.1341	.1273	
0.80	.1360	.1613	.1182	.1159	
0.85	.1160	.1455	.1000	.1000	
0.90	.0930	.1204	.0727	.0795	
0.95	.0680	.0841	.0454	.0477	
1.00	.0386	.0489	.0227	.0227	

4.) $n_e(0) = 2.44 \cdot 10^{14} \text{ cm}^{-3}$ 2.5 T

norm. n _{d1} /F _i	O1	O3	W1	W3	reff-Param 0.187 ne(0)-Param 2.44
0.05	.0000	.0000	.0000	.0000	
0.10	.0023	.0000	.0000	.0045	
0.15	.0114	.0040	.0113	.0159	
0.20	.0341	.0114	.0368	.0341	
0.25	.0682	.0023	.0841	.0682	
0.30	.1022	.0545	.1455	.1364	
0.35	.1360	.0818	.1818	.1932	
0.40	.1700	.1023	.1841	.2295	
0.45	.1930	.1341	.1705	.2250	
0.50	.1980	.1636	.1500	.1886	
0.55	.1930	.1773	.1341	.1545	
0.60	.1820	.1795	.1182	.1250	
0.65	.1477	.1750	.1023	.0977	
0.70	.1136	.1477	.0932	.0795	
0.75	.0910	.1227	.0841	.0614	
0.80	.0680	.1000	.0750	.0500	
0.85	.0545	.0818	.0591	.0352	
0.90	.0364	.0682	.0409	.0227	
0.95	.0250	.0432	.0273	.0136	
1.00	.0136	.0204	.0114	.0068	

5.) $n_e(0) = 2.66 \cdot 10^{14} \text{ cm}^{-3}$

/ 2.5 T

reff-Param
0.169
Param
2.66

norm. n _{d1} /F _i	O1	O3	W1	W3
0.05	.0023	.0023	.0045	.0023
0.10	.0114	.0090	.0432	.0409
0.15	.0455	.0250	.1022	.0795
0.20	.0909	.0523	.1705	.2227
0.25	.1477	.0818	.1977	.2410
0.30	.1909	.1793	.2068	.2410
0.35	.2000	.1523	.2000	.2273
0.40	.1977	.1795	.1750	.1932
0.45	.1886	.1818	.1477	.1591
0.50	.1727	.1750	.1136	.1364
0.55	.1522	.1636	.0954	.1045
0.60	.1320	.1500	.0954	.0795
0.65	.1160	.1386	.0100	.0182
0.70	.1040	.1250	.0977	.0523
0.75	.0860	.1136	.0910	.0432
0.80	.0700	.0977	.0750	.0318
0.85	.0560	.0795	.0591	.0227
0.90	.0410	.0591	.0455	.0148
0.95	.0250	.0386	.0284	.0090
1.00	.0114	.0227	.0159	.0045

6.) $n_e(0) = 0.34 \cdot 10^{14} \text{ cm}^{-3}$

/ 1.25T

***** reff-Param
0.178
ne(0)-Param
0.34

norm. n _{d1} /F _i	O1	O3	W1	W3
0.05	.0079	.0068	.0009	.0068
0.10	.0205	.0204	.0250	.0227
0.15	.0261	.0261	.0386	.0364
0.20	.0295	.0341	.0477	.0477
0.25	.0330	.0398	.0545	.0568
0.30	.0375	.0511	.0591	.0591
0.35	.0432	.0489	.0636	.0682
0.40	.0568	.0727	.0750	.0795
0.45	.0727	.0841	.0909	.0977
0.50	.1023	.1023	.1068	.1136
0.55	.1272	.1250	.1227	.1272
0.60	.1500	.1455	.1386	.1591
0.65	.1727	.1602	.1500	.1682
0.70	.1841	.1682	.1636	.1704
0.75	.1840	.1750	.1727	.1636
0.80	.1772	.1730	.1727	.1500
0.85	.1636	.1591	.1500	.1250
0.90	.1386	.1182	.1182	.1022
0.95	.0955	.0841	.0818	.0704
1.00	.0432	.0511	.0432	.0454

7.) $ne(0) = 0.68 \cdot 10^{14} \text{ cm}^{-3}$ / 1.25T

norm. ndl/F_i	O1	O3	W1	W3	reff-Param: 0.178 ne(0)-Param 0.68
0.05	.0091	.0068	.0090	.0113	
0.10	.0200	.0227	.0341	.0341	
0.15	.0295	.0318	.0545	.0523	
0.20	.0363	.0409	.0682	.0682	
0.25	.0454	.0477	.0772	.0841	
0.30	.0545	.0568	.0909	.0954	
0.35	.0682	.0682	.1000	.1068	
0.40	.0818	.0841	.1136	.1159	
0.45	.1023	.1131	.1216	.1250	
0.50	.1205	.1318	.1318	.1318	
0.55	.1477	.1500	.1364	.1409	
0.60	.1818	.1636	.1398	.1466	
0.65	.1886	.1681	.1398	.1500	
0.70	.1773	.1636	.1363	.1500	
0.75	.1591	.1545	.1273	.1273	
0.80	.1364	.1386	.1182	.1045	
0.85	.1113	.1204	.1045	.0841	
0.90	.0886	.0955	.0864	.0636	
0.95	.0636	.0659	.0591	.0432	
1.00	.0341	.0341	.0295	.0250	

8.) $ne(0) = 1.02 \cdot 10^{14} \text{ cm}^{-3}$ / 1.25T

norm. ndl/F_i	O1	O3	W1	W3	reff-Param: 0.178 ne(0)-Param 1.02
0.05	.0023	.0023	.0114	.0159	
0.10	.0114	.0091	.0250	.0522	
0.15	.0159	.0181	.0454	.0795	
0.20	.0227	.0227	.0614	.1022	
0.25	.0318	.0341	.0818	.1159	
0.30	.0455	.0454	.1000	.1193	
0.35	.0636	.0591	.1159	.1227	
0.40	.0841	.0818	.1341	.1273	
0.45	.1091	.1022	.1454	.1295	
0.50	.1295	.1250	.1500	.1341	
0.55	.1568	.1454	.1500	.1341	
0.60	.1750	.1669	.1480	.1318	
0.65	.1818	.1773	.1432	.1227	
0.70	.1795	.1773	.1341	.1068	
0.75	.1704	.1705	.1159	.0932	
0.80	.1500	.1500	.1034	.0841	
0.85	.1227	.1295	.0818	.0682	
0.90	.0909	.1091	.0636	.0545	
0.95	.0590	.0705	.0386	.0386	
1.00	.0318	.0386	.0205	.0250	

9.) $ne(0) = 1.36 \cdot 10^{14} \text{ cm}^{-3} / 1.25T$

norm. ndl/Fi	O1	O3	W1	W3
0.05	.0011	.0068	.0114	.0136
0.10	.0114	.0136	.0545	.0500
0.15	.0182	.0205	.0841	.0795
0.20	.0273	.0295	.1023	.1022
0.25	.0341	.0364	.1159	.1182
0.30	.0477	.0500	.1160	.1318
0.35	.0636	.0659	.1136	.1420
0.40	.0886	.0795	.1136	.1500
0.45	.1091	.0977	.1147	.1500
0.50	.1364	.1227	.1159	.1409
0.55	.1636	.1500	.1182	.1341
0.60	.1772	.1647	.1205	.1227
0.65	.1818	.1750	.1216	.1136
0.70	.1818	.1795	.1227	.1023
0.75	.1750	.1682	.1148	.0864
0.80	.1545	.1477	.1034	.0727
0.85	.1136	.1227	.1023	.0568
0.90	.0818	.1000	.0841	.0432
0.95	.0500	.0727	.0523	.0273
1.00	.0273	.0409	.0329	.0136

reff-Param
0.178
ne(0)-Param
1.36

10.) $ne(0) = 1.80 \cdot 10^{14} \text{ cm}^{-3} / 1.25T$

norm. ndl/Fi	O1	O3	W1	W3
0.05	.0023	.0045	.0182	.0204
0.10	.0114	.0125	.0682	.0795
0.15	.0216	.0205	.0909	.1205
0.20	.0318	.0295	.1045	.1477
0.25	.0455	.0386	.1113	.1682
0.30	.0591	.0523	.1205	.1795
0.35	.0773	.0659	.1227	.1830
0.40	.0932	.0841	.1227	.1659
0.45	.1182	.1091	.1227	.1364
0.50	.1432	.1363	.1216	.1136
0.55	.1591	.1591	.1205	.0909
0.60	.1659	.1705	.1205	.0841
0.65	.1681	.1750	.1170	.0826
0.70	.1659	.1705	.1113	.0795
0.75	.1568	.1636	.1068	.0705
0.80	.1364	.1477	.0954	.0614
0.85	.1136	.1227	.0795	.0523
0.90	.0841	.1000	.0636	.0443
0.95	.0545	.0610	.0432	.0295
1.00	.0307	.0295	.0193	.0136

reff-Param
0.178
ne(0)-Param
1.80